

This document is confidential and is proprietary to the American Chemical Society and its authors. Do not copy or disclose without written permission. If you have received this item in error, notify the sender and delete all copies.

### Spectroscopic and thermodynamic study of Chrysin and Quercetin complexes with Cu(II)

Journal:	<i>Journal of Chemical &amp; Engineering Data</i>
Manuscript ID	je-2015-008378
Manuscript Type:	Article
Date Submitted by the Author:	30-Sep-2015
Complete List of Authors:	Muñoz, Vanesa; San Luis National University, Physical Chemistry Area - Department of Chemistry; Instituto de Química de San Luis INQUISAL (CONICET- UNSL) Ferrari, Gabriela; San Luis National University, Physical Chemistry Area - Department of Chemistry; Instituto de Química de San Luis INQUISAL (CONICET- UNSL) Sancho, Matias; Universidad Nacional de San Luis, Chemistry Department; Instituto Multidisciplinario de Investigaciones Biológicas IMIBIO (CONICET- UNSL) Montaña, Maria; San Luis National University, Physical Chemistry Area - Department of Chemistry

SCHOLARONE™  
Manuscripts

# Spectroscopic and thermodynamic study of Chrysin and Quercetin complexes with Cu(II)

Vanesa A. Muñoz<sup>a,b</sup>, Gabriela V. Ferrari<sup>a,b</sup>, Matias I. Sancho<sup>a,c</sup>, M. Paulina Montaña<sup>a,b\*</sup>

*a* Área de Química Física, Facultad de Química, Bioquímica y Farmacia, Universidad Nacional de San Luis, Lavalle 1155, D5700HZW, San Luis, Argentina

*b* Instituto de Química de San Luis INQUISAL (CONICET- UNSL)

*c* Instituto Multidisciplinario de Investigaciones Biológicas IMIBIO (CONICET-UNSL)

KEYWORDS: Chrysin – Copper(II) complex, DFT, Quercetin – Copper(II) complex, Stability Constants.

ABSTRACT: Chrysin and Quercetin are natural polyphenolic compounds which present benefits in human health because of their biological properties. These flavonoids also have the capacity to complex a wide variety of metallic ions which could affect their bioactivity. In order to assay the complexant capacity of flavonoids, the metallic ion Cu(II) was selected. Formation of two flavonoids-Cu(II) complexes in ethanolic solutions were studied and both complexes presented 2:1 L:M stoichiometries. The apparent formation constants for Quercetin-Cu(II) are higher than those of Chrysin-Cu(II) ones, suggesting that Quercetin may act as a better analytical reagent than Chrysin. A molecular modeling analysis was performed in order to gain insight into the spectroscopic properties of the complexes.

## INTRODUCTION

Flavonoids are a family of varied polyphenolic compounds widely distributed in nature, with physicochemical properties of scientific interest. These compounds present benefits in human health because of their biological properties which include activity against HIV<sup>1</sup>, influenza virus<sup>2</sup> and bacteria<sup>3</sup>. Flavonoids also show antithrombotic<sup>4</sup>, anti-inflammatory<sup>5</sup>, antitumoral<sup>6</sup>, antiallergic<sup>7</sup> and antioxidant<sup>8</sup> effects. Latest scientific researches confer antioxidant activity of flavonoids to their skill for linking with enzymes<sup>9</sup>, DNA<sup>10</sup>, as well as quenching reactive oxygen species<sup>11</sup>. Due to this last property several effects on diseases as diabetes<sup>12</sup>, cancer<sup>13</sup>, heart diseases<sup>14</sup>, stomachal and duodenal ulcers<sup>15</sup>, among others, have been described. In particular Chrysin or 5,7-dihydroxyflavone, a natural flavone which may be found in propolis and plants<sup>16</sup>, shows several biological properties that includes the reduction of melanoma cell proliferation<sup>17</sup>.

From some time, authors have reported flavonoids capacity to complex a wide variety of metallic ions<sup>18,19</sup>. According to these investigations, those flavones with a hydroxyl group on C3 or C5 are able to form stable metallic complexes, while those with ortho-hydroxylated systems in B-ring form labile complexes. The biological activity of flavonoids is believed to increase when they are coordinated with metallic ions. The experimental results suggest that the metallic ions significantly change chemical properties of the free flavonoid, e.g. a decrease of its oxidation potentials, furthermore the complexes show higher antioxidant activity compared to the free ligands<sup>20,21</sup>.

Flavonoids also may be used as analytical reagents for complexing diverse metallic ions. A spectrofluorimetric method have been developed for determining trace levels of zinc by means of the complex formation between the metallic ion and 3-hydroxyflavone<sup>22</sup>. Flavonoid complexing

1  
2  
3 capacity may influence on its bioactivity by acting as carriers and regulators of metal  
4  
5 concentration<sup>23</sup>. Many researchers have synthesized metal-flavonoid complexes as solid and have  
6  
7 been able to characterize them by means of spectroscopic data, thermal analysis, among others.  
8  
9 However, there are few data on the flavonoids ability of complexation in solution and even fewer  
10  
11 data regarding the thermodynamic study of these complexes, which are important in order to  
12  
13 characterize them.  
14  
15

16  
17  
18 Cu(II) and Fe(II) metallic ions have an important role as cofactors in living systems, and  
19  
20 according to this, the presence of competitive complexing agents could affect their bioactivity<sup>24</sup>.  
21  
22 Studies carried out by Baccan et. al. describe that Rutin and Quercetin are able to complex Fe(II)  
23  
24 in blood plasma and transfer it to transferrin. Since the complex Quercetin-Fe(II) can traverse  
25  
26 biological membranes it is possible to use this flavone as chelant agent in redistributing-Fe  
27  
28 therapy<sup>25</sup>.  
29  
30  
31

32  
33 In order to assay the complexant capacity of flavonoids, as stated above, the metallic ion Cu(II)  
34  
35 was selected. Copper is a transition metal useful due to a wide variety of chemical, physical,  
36  
37 mechanical and electrical properties. Its compounds are mainly used in agriculture, specially as  
38  
39 fungicides and insecticides<sup>26</sup>, but are also used in inkjet printing<sup>27</sup>, galvanoplastic nucleation<sup>28</sup>,  
40  
41 catalysis<sup>29</sup>, etc. Copper is also essential in the regulation of oxide-reduction reactions, transport  
42  
43 and in the use of Fe in metabolic processes<sup>30</sup>.  
44  
45  
46  
47

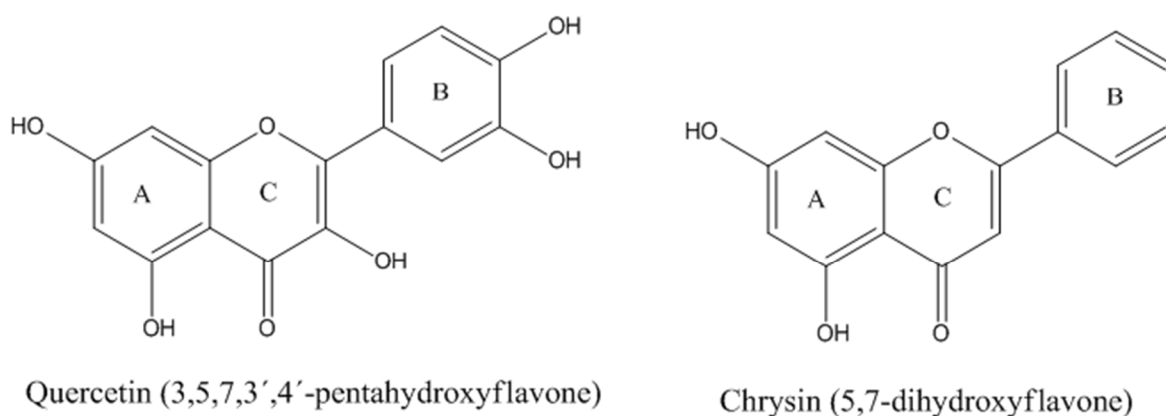
48  
49 The aim of this work is, first, to determine the stoichiometry of the complexes between two  
50  
51 flavonoids (Quercetin and Chrysin) with Cu(II) in solution, and afterwards, evaluate their  
52  
53 apparent stability constants and the thermodynamic parameters associated to the formation  
54  
55 reaction. Furthermore, the theoretical formation constants of Chrysin-Cu(II) and Quercetin-  
56  
57  
58  
59  
60

1  
2  
3 Cu(II) complexes are also evaluated from DFT calculations. It is necessary a computational TD-  
4  
5  
6 DFT study to compare the simulated UV-Vis absorption spectra of the complexes in ethanolic  
7  
8 solution with the experimental ones.  
9  
10  
11  
12  
13

## 14 MATERIALS AND METHODS

### 15 MATERIALS

16  
17  
18 The structures and numbering system of the two flavones studied are shown in Figure 1.  
19  
20  
21  
22 The structures and numbering system of the two flavones studied are shown in Figure 1.  
23  
24 Quercetin and Chrysin were purchased from Sigma. The Cu(II) solutions were obtained  
25  
26 dissolving the salt  $\text{CuSO}_4 \cdot 5\text{H}_2\text{O}$ , provided by Merck. Ethanol spectroscopic grade was used as  
27  
28 solvent in all assays performed. Buffers were prepared using the following drugs:  $\text{KH}_2\text{PO}_4$  (p.a  
29  
30 Berna),  $\text{Na}_2\text{HPO}_4 \cdot 12\text{H}_2\text{O}$  (p.a Mallinckrodt),  $\text{Na}_2\text{B}_4\text{O}_7 \cdot 10\text{H}_2\text{O}$  (p.a Merck),  $\text{KC}_8\text{H}_5\text{O}_4$  (p.a  
31  
32 Tetrahedron).  
33  
34  
35  
36  
37  
38  
39  
40  
41  
42  
43  
44  
45  
46  
47  
48  
49  
50  
51



52 **Figure 1.** Chemical structure of Quercetin and Chrysin.  
53  
54  
55  
56  
57  
58  
59  
60

## APPARATUS AND METHODS

An Agilent 8454 diode-array spectrophotometer provided with an AGILENT 89090A temperature controller was used to record the ligands and their complexes spectra and also to measure absorbances required.

The FT-IR spectra of the free ligands and the metallic complexes were registered in the 4000 – 400  $\text{cm}^{-1}$  region using a Shimadzu IR Affinity-1 spectrophotometer, with a spectral resolution of 2  $\text{cm}^{-1}$ . Since obtaining of complexes in solid state was not possible, spectra were recorded after deposition of the sample solution on the surface of KBr pellets. This procedure has been successfully applied for flavonoids metallic complexes<sup>31</sup>.

The stoichiometries of the complexes formed were determined using Yoe-Jones method<sup>32</sup>. This spectrophotometric method requires the preparation of a set of solutions varying the ligand concentration [L], but keeping constant the metallic ion concentration [M]. The absorbance, A, of these solutions is measured at a wavelength where only complex absorbs and used to plot a graphic of A vs [L]/[M]. The intersection points between the straight lines of the experimental data indicate the ligand:metal L:M molar ratio.

The apparent formation constant K of the complexes were determined using a graphic linear method developed by Debattista et. al.<sup>33</sup>, which can be applied to both mono and poli nuclear complexes. This method only requires the reactants analytical concentration and the absorbances of the complex solutions in the equilibrium. These data are used to plot the following expression valid for a  $L_nM$  complex:

$$a_j^n + n^2 \cdot a_j^{n-1} \cdot b_j = \frac{(a_r^n + n^2 \cdot a_r^{n-1} \cdot b_r + K')(A - A_L)_r}{(a_r^n b_r)} \cdot \frac{a_j^n b_j}{(A - A_L)_j} - \frac{1}{K} \quad (1)$$

where  $a$  is ligand molar concentration,  $b$ , metallic ion molar concentration,  $r$  and  $j$  indicate two solutions in equilibrium,  $A$  is the reacting solution absorbance meanwhile  $A_L$  is the absorbance of the ligand solution,  $K$  is the apparent formation constant and  $K' = 1/K$ . The apparent formation constant can be calculated from the intercept of the  $(a_j^n + n^2 \cdot a_j^{n-1} \cdot b_j)$  vs.  $\left(\frac{a_j^n b_j}{(A - A_L)_j}\right)$  plot.

## COMPUTATIONAL DETAIL

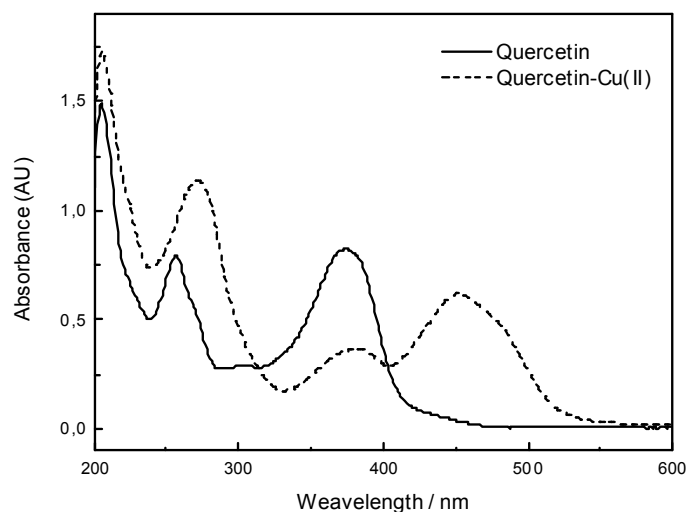
The molecular geometries of Chrysin, Quercetin and its 1:2 complexes with  $\text{Cu}^{2+}$  were fully optimized using the unrestricted DFT functional UB3LYP<sup>34,35</sup>. For the Cu atom the Los Alamos double- $\xi$  (LANL2DZ) effective core potential was implemented and for the rest of the atoms the 6-31+G(d,p) basis set was used. The vibrational frequencies of the free ligands and the complexes were performed for the thermodynamic analysis. No imaginary frequencies were found. The solvent effect on the gas-phase optimized structures was analyzed using the polarizable continuum model with the integral equation formalism (IEF-PCM)<sup>36</sup> and the UAHF radii set were employed to build the solvent cavity. The vertical excitation energies and the corresponding absorption wavelengths of the complexes were calculated within the non-equilibrium time-dependent density functional theory (TD-DFT) framework<sup>37</sup>. Four functional were used in these calculations: the exchange-correlation hybrids B3LYP<sup>34,35</sup>, PBE0<sup>38,39</sup> and M06<sup>40</sup>, and the Long-range corrected functional CAM-B3LYP<sup>41</sup>. Finally, the electronic transitions were analyzed using Natural Transition Orbitals (NTO)<sup>42</sup>, which provides a good

1  
2  
3 representation of the electronic transitions in terms of single particles. All the calculations were  
4  
5 performed with the Gaussian 09 software package<sup>43</sup>.  
6  
7  
8  
9

## 10 11 12 RESULTS AND DISCUSSION

### 13 14 15 1. SPECTROSCOPIC ANALYSIS

16  
17  
18 The formation of two hydroxyflavones–Cu(II) complexes were noticed by yellow color  
19  
20 intensification of the flavonoid solutions after adding the metallic ion solution. This occurs due  
21  
22 to a bathochromic shift and was confirmed by recording the spectra of the ligand solution and the  
23  
24 same solution after adding Cu(II) solution (see Figure 2).  
25  
26  
27  
28  
29  
30



31  
32  
33  
34  
35  
36  
37  
38  
39  
40  
41  
42  
43  
44  
45  
46  
47  
48  
49  
50  
51 **Figure 2.** Spectra of Quercetin and Quercetin-Cu(II) complex

52  
53  
54  
55 The UV-Vis absorption spectra of the flavones show two characteristic absorption bands related  
56  
57 to  $\pi \rightarrow \pi^*$  transitions in their three-aromatic rings system. The absorption band in the (300-400)  
58  
59  
60



1  
2  
3 nm range is related to B-ring absorption (cinnamoyl system, Band I), while the absorption  
4  
5 between (250-300) nm corresponds to A-ring absorption (benzoyl system, Band II). In Figure 2  
6  
7 are shown the spectra obtained for Quercetin solution with and without Cu(II). Band I in  
8  
9 complex spectrum is shifted to longer wavelength compared to that of the free flavonoid. The  
10  
11 shifting could be explained considering the increased conjugation of the system caused by a new  
12  
13 ring formation involving the 3-OH and 4-oxo group. The new band centered at 400 nm can be  
14  
15 attributed to the flavonoid-metallic ion complex formation, considering that neither the metallic  
16  
17 ion nor the ligand absorbs in that wavelength range. The same explanations are useful to describe  
18  
19 Chrysin-Cu(II) spectra (not shown). In addition, the systems Quercetin-Cu(II) and Chrysin-  
20  
21 Cu(II) show a diminished absorption in this band, which evidence the complex formation.  
22  
23  
24  
25  
26  
27  
28 Since Quercetin has three possible sites to coordinate with Cu(II) ion, a molecular modeling  
29  
30 analysis was performed in order to gain insight into the spectroscopic properties of the  
31  
32 complexes.  
33  
34  
35  
36  
37  
38

## 39 2. THERMODYNAMIC STUDIES OF FLAVONOID-CU(II) COMPLEXES

40  
41  
42 Stoichiometries of formed complexes were determined by Yoe-Jones method. Both complexes  
43  
44 exhibited 2:1 ligand:metal molar composition (see Figure 3, A and B Insets). Considering this  
45  
46 information it is possible to use Debattista *et. al.* method<sup>33</sup> to determine the apparent formation  
47  
48 constant. Figure 3 shows the plots for both systems studied and Table 1, the determined ln K  
49  
50 values.  
51  
52  
53  
54  
55  
56  
57  
58  
59  
60

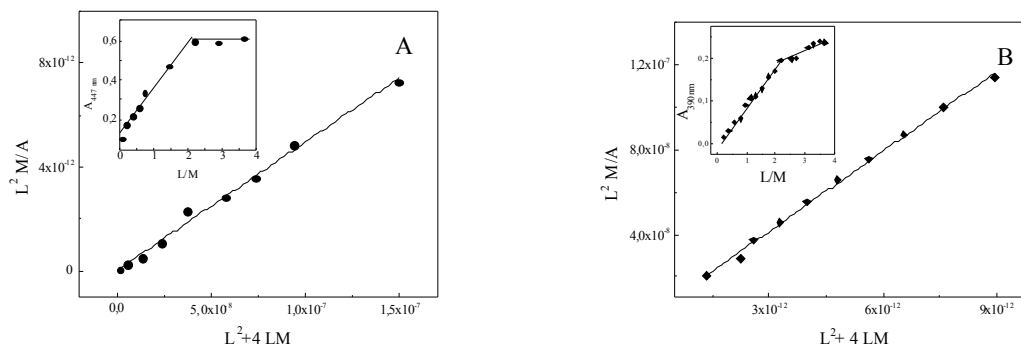


**Figure 3. A:** Equilibrium constant determination at 25 °C and stoichiometry determination (Inset) of Quercetin-Cu(II) complex. **B:** Example of equilibrium constant determination at 25 °C and stoichiometry determination (Inset) of Chrysin-Cu(II) complex.


**Table 1.** Apparent formation constant values and thermodynamic parameters of Chrysin-Cu(II) and Quercetin-Cu(II) complexes at different temperatures.

System	Ln K				$\Delta H$ / kJ mol <sup>-1</sup>	$\Delta S$ / J mol <sup>-1</sup> K <sup>-1</sup>
	15 °C	20 °C	25 °C	30 °C		
Chrysin-Cu(II)	18.9	19.1	19.4	19.7	39	291
Quercetin-Cu(II)	20.7	21.0	22.5	22.9	118	582

Errors of all determination are comprised between  $7 \times 10^{-3}$  and  $8 \times 10^{-2}$ .

In order to estimate thermodynamic parameters of the complexation reaction, apparent formation constants at different temperatures (15, 20, 25 and 30 °C) were determined. By means of the

Vant' Hoff equation ( $\ln K = -\frac{\Delta H}{RT} + \frac{C}{T}$ , with  $C =$  integration constant), the standard enthalpy and entropy of the process were determined (Figure 4). The thermodynamic data calculated by means of the Vant' Hoff equation are listed in Table 1.

The stability constant values for Quercetin-Cu(II) and Chrysin-Cu(II) systems decrease with increasing temperature, according to other studied systems 

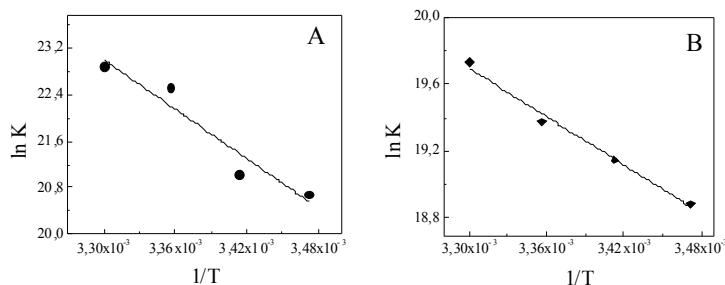
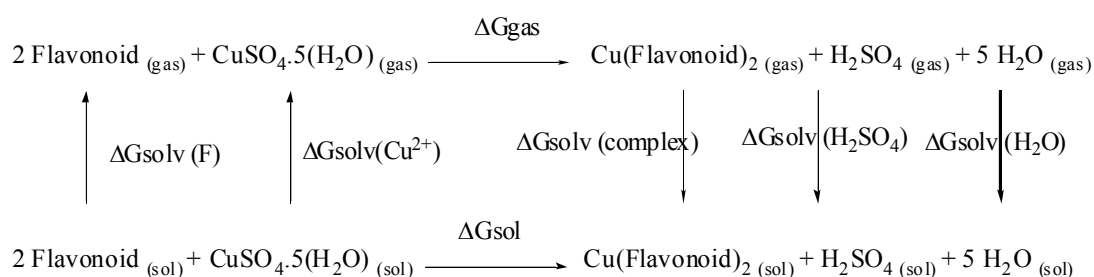


**Figure 4.** Graphical representation of Vant' Hoff's equation for Quercetin-Cu(II) complex (A) and for Chrysin-Cu(II) complex (B).

The theoretical formation constants ( $K_{CT}$ ) of the Chrysin-Cu(II) and the Quercetin-Cu(II) complexes were also evaluated from DFT calculations. The  $\Delta G_{sol}$  values necessary to calculate  $K_{CT}$  were obtained using a procedure based on a thermodynamic cycle. For this purpose, the following reaction scheme was proposed:



In the scheme depicted above, Flavonoid is Chrysin or Quercetin,  $\Delta G_{gas}$  and  $\Delta G_{sol}$  are the Gibbs energy changes of the reaction in gas phase and in ethanolic solution, respectively and  $\Delta G_{solv}$  is the Gibbs energy change of solvation. The Gibbs energy in gas phase at 298 K

( $G^{\circ}_{298}$ ) of all the structures present in the reaction scheme was calculated with the following equation<sup>45</sup>:

$$G^{\circ}_{298} = E + ZPVE + H_{corr} - T S^{\circ}_{298} \quad (2)$$

where  $E$  is the gas phase total energy,  $ZPVE$  is the zero-point vibrational energy,  $H_{corr}$  is the thermal correction to enthalpy and  $S^{\circ}_{298}$  is the entropy at 298 K. In the same way, the  $\Delta G_{solv}$  and the Gibbs energy in solution ( $G^{\circ}_{sol}$ ) of each structure were calculated using the following expressions:

$$\Delta G_{solv} = E_{PCM} - E \quad (3)$$

$$G_{sol} = G^{\circ}_{298} + \Delta G_{solv} \quad (4)$$

In Eq. (3)  $E_{PCM}$  is the total energy in solution calculated with the polarizable continuum model. With Eqs (2-4), the  $\Delta G_{sol}$  of the complexation reaction (and the corresponding  $\ln K_{CT}$ ) can be estimated as the difference between the  $G_{sol}$  of the products and the  $G_{sol}$  of the reactants. From the  $\Delta G_{sol}$ , the  $\ln K_{CT}$  can be obtained.


The optimized geometries of Quercetin-Cu(II) and Chrysin-Cu(II) complexes are illustrated in Figure 5. Since Quercetin presents three different chelating sites for Cu(II), three different structures of the Quercetin-Cu(II) complex were proposed, where the flavonoid coordinates with copper in: *i*) the 3-OH-4-Oxo group; *ii*) the 5-OH-4-Oxo group and *iii*) the catechol group. The calculated  $\ln K_{CT}$  for these complexes (and the  $\Delta G_{sol}$ ) are reported in Table 2.

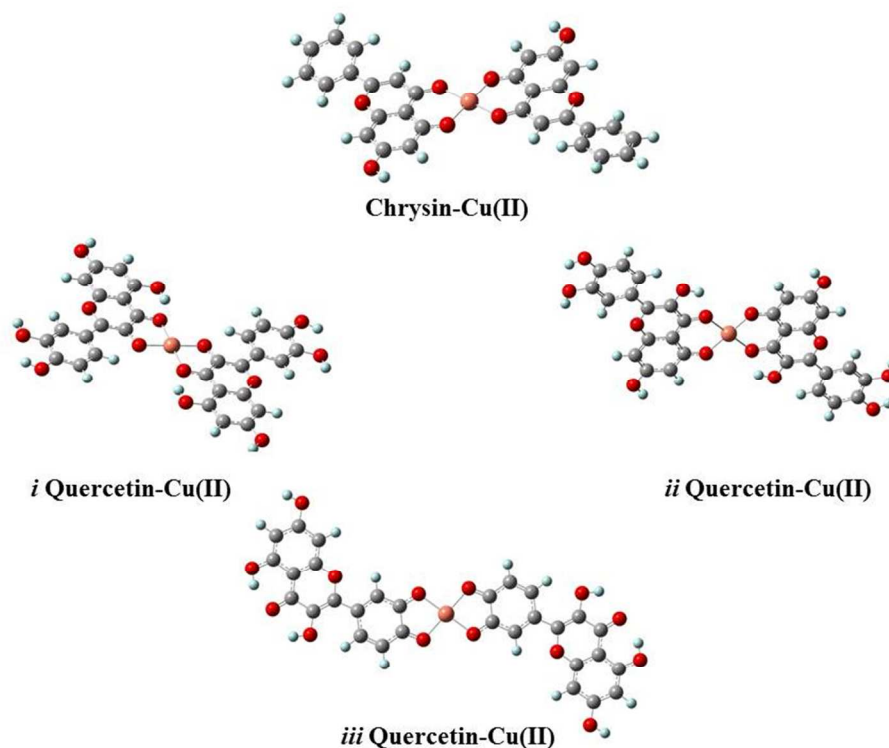


**Figure 5.** Optimized geometries of Quercetin-Cu(II) and Chrysin-Cu(II) complexes.

**Table 2.** Gibbs energy changes (in kJ/mol) in gas phase and solution and Formation constants of the studied flavonoid-Cu(II) complexes calculated at DFT level of theory.

	Chrysin-Cu(II)	<i>i</i> Quercetin-Cu(II)	<i>ii</i> Quercetin-Cu(II)	<i>iii</i> Quercetin-Cu(II)
$\Delta G_{\text{gas}}$	-8.31	- 18.00	-9.31	3392
$\Delta G_{\text{sol}}$	-33.22	-41.03	-43.29	3288
$K_{\text{CT}}$	$6.61 \times 10^5$	$1.54 \times 10^7$	$3.85 \times 10^7$	$2.43 \times 10^{-58}$
$\text{Ln } K_{\text{CT}}$	13.40	16.55	17.47	-132.6

1  
2  
3 From these values it can be observed that the predicted stability of Quercetin-Cu(II) is higher  
4 than the stability of Chrysin-Cu(II), in agreement with the experimental results. Moreover, for  
5 Quercetin-Cu(II) complex the site *iii* presents a considerably lower stability than sites *i* and *ii*.  
6  
7 These last two sites, which are similar from a structural point of view, exhibit comparable  $\ln K_{CT}$   
8 values, being the site *ii* more stable only by 2.26 kJ/mol than site  or this reason, the DFT  
9 results suggests that the complexation of  $Cu^{2+}$  by Quercetin takes place in the 3-OH-4-oxo and 5-  
10 OH-4-oxo sites; and the catechol group is the less effective chelating site under the adopted  
11 conditions. From the evaluation of the theoretical formation constants, it is not possible to  
12 establish a preferential site between complexes *i* and *ii* since the energy difference is too low.  
13  
14  
15  
16  
17  
18  
19  
20  
21  
22  
23  
24  
25  
26  
27

### 28 3. TD-DFT RESULTS

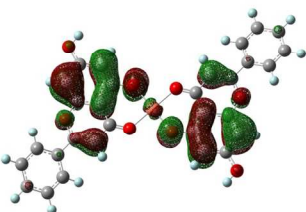
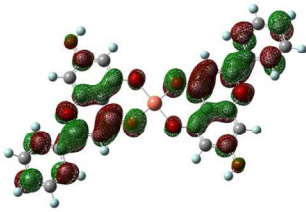
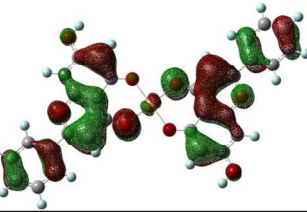
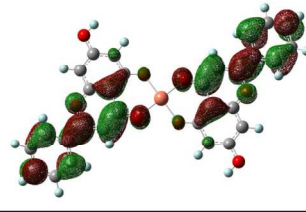
29  
30  
31 A computational TD-DFT study was also performed in order to compare the simulated UV-Vis  
32 absorption spectra of the complexes in ethanolic solution with the experimental ones. For this  
33 aim, four functional were employed, B3LYP, PBE0, M06 and CAM-B3LYP and the IEF-PCM  
34 formalism was applied to simulate the solvent effect. In Table 3, the predicted absorption  
35 wavelengths ( $\lambda_{TD-DFT}$ ) and the oscillator strengths obtained with this methodology are reported.  
36 For the Chrysin-Cu(II) complex, the calculated  $\lambda_{TD-DFT}$  with the PBE0 functional is very close to  
37 the experimental value (underestimated by 3 nm), the B3LYP  $\lambda_{TD-DFT}$  is moderately well  
38 predicted, while the  $\lambda_{TD-DFT}$  values obtained with the functionals M06 and CAM-B3LYP exhibit  
39 large errors compared to the experimental  $\lambda$ . In the case of the Quercetin-Cu(II) complex, the  
40 spectra of the three proposed structures were calculated. These results show very large errors in  
41 the  $\lambda_{TD-DFT}$  for the chelating site *iii*, indicating this site as the least probable, in agreement with  
42  
43  
44  
45  
46  
47  
48  
49  
50  
51  
52  
53  
54  
55  
56  
57  
58  
59  
60


the thermodynamic analysis. Moreover, by examining the calculated  $\lambda_{\text{TD-DFT}}$  of sites *i* and *ii*, it can be seen that the  $\Delta\lambda$  values obtained for the former structure are lower than the  $\Delta\lambda$  of site *ii* with all the functionals (except the M06). Particularly, the  $\Delta\lambda$  of site *i* complex calculated with B3LYP and PBE0 are almost the half of the  $\Delta\lambda$  values of site *ii* complex. For this reason, the coordination site *i* seems to be the preferred one for the complexation of Cu(II) by Quercetin in ethanol. However, the coordination site *ii* cannot be completely discarded, and the formation of the complex involving this site may occur to some extent. The coexistence of both forms for Quercetin metal complexes has been previously reported<sup>46,47</sup>.

**Table 3.** Calculated ( $\lambda_{\text{TD-DFT}}$ ) wavelengths (in nm) for flavonoid-Cu(II) complexes from TD-DFT/PCM simulations.  $\lambda_{(\text{exp})}$  is the experimental wavelength of the complex, *f* the oscillator strength and  $\Delta\lambda$  the difference between the calculated and experimental wavelengths in absolute value.

Complex	$\lambda_{(\text{exp})}$	B3LYP			PBE0		
		$\lambda_{\text{TD-DFT}}$	<i>f</i>	$\Delta\lambda$	$\lambda_{\text{TD-DFT}}$	<i>f</i>	$\Delta\lambda$
Chrysin-Cu(II)	395.0	413.1	0.435	18.1	392.0	0.494	3.0
<i>i</i> -Quercetin-Cu(II)	450.0	455.8	0.490	6.8	433.9	0.924	15.1
<i>ii</i> -Quercetin-Cu(II)	450.0	435.6	1.099	13.4	419.3	1.182	29.7
<i>iii</i> -Quercetin-Cu(II)	450.0	478.6	0.775	29.6	735.7	0.129	287
Complex	$\lambda_{(\text{exp})}$	M06			CAM-B3LYP		
		$\lambda_{\text{TD-DFT}}$	<i>f</i>	$\Delta\lambda$	$\lambda_{\text{TD-DFT}}$	<i>f</i>	$\Delta\lambda$
Chrysin-Cu(II)	395.0	422.2	0.665	27.2	435.6	0.125	40.6
<i>i</i> -Quercetin-Cu(II)	450.0	430.6	0.815	18.4	399.8	1.337	49.2
<i>ii</i> -Quercetin-Cu(II)	450.0	435.5	1.144	13.5	385.4	1.458	63.6
<i>iii</i> -Quercetin-Cu(II)	450.0	502.2	0.723	53.2	422.2	0.2529	26.8

The nature of the electronic transitions involved in the UV-Vis absorption bands of the complexes were analyzed using Natural Transition Orbitals (NTOs). This approximation provides a compact representation of the transition density between the ground and excited states in terms of an expansion into single-particle transitions<sup>42</sup>, where occupied and unoccupied orbitals are referred as “hole” and “electron” respectively. The NTOs were constructed with the PBE0 functional, since good results were obtained in the calculation of the complexes absorption wavelengths.

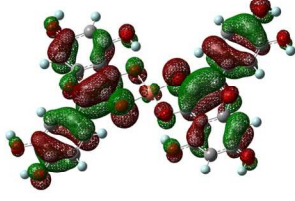
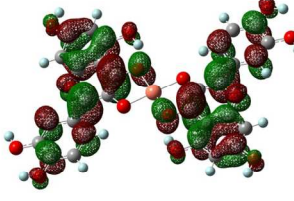
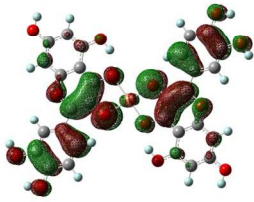
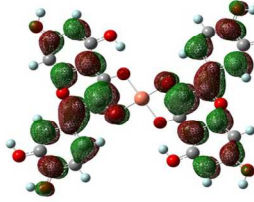
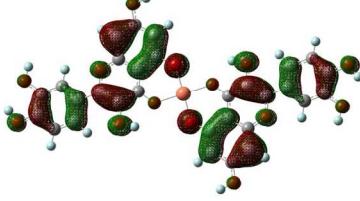
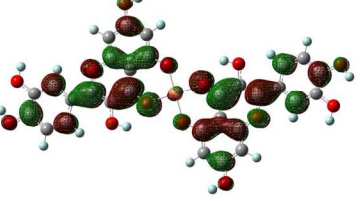
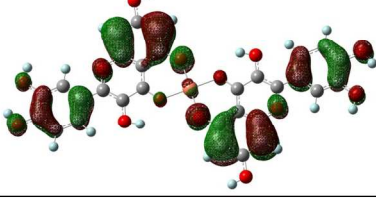
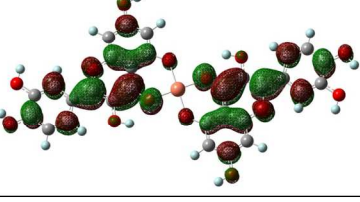
Chrysin-Cu(II)	Hole	Electron
T11( $\beta$ ) $\lambda_{\text{TD-DFT}} = 392 \text{ nm}$ $f=0.494$		
T36( $\beta$ ) $\lambda_{\text{TD-DFT}} = 294 \text{ nm}$ $f=0.289$		

**Figure 6.** Natural Transition Orbitals (NTOs) for the Chrysin-Cu(II) complex in the absorption bands at 395 and 271 nm. For each state, the calculated wavelength ( $\lambda_{\text{TD-DFT}}$ ) and the oscillator strength  $f$  are listed 

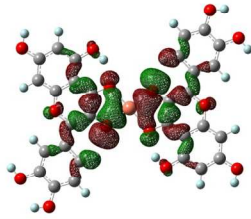
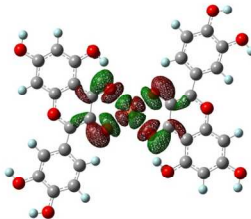
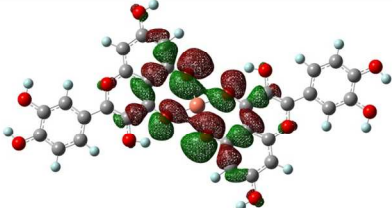
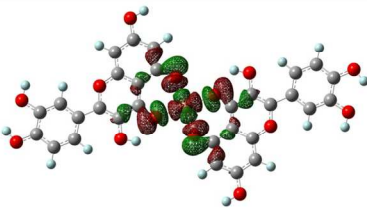
The NTOs of the Chrysin-Cu(II) complex (Figure 6) indicates that the absorption band located at 395 nm ( $\lambda_{\text{TD-DFT}} = 392 \text{ nm}$ ) the transition correspond to an intraligand charge transfer (ILCT) with a small contribution of a metal-to-ligand charge transfer (MLCT). It can be observed that



1  
2  
3 the ILCT takes place from rings A and C of Chrysin to the whole ligand. The other absorption  
4 band ( $\lambda_{\text{exp}}$  271 nm,  $\lambda_{\text{TD-DFT}}$  = 293 nm) also corresponds to a mixed MLCT/ILCT transition. For  
5  
6 the Quercetin-Cu(II) complex only sites i and ii were considered in the analysis, taking into  
7  
8 account the thermodynamic and TDDFT results. The NTOs calculated for the site i Quercetin-  
9  
10 Cu(II) complex (Figure 3) show a main  $\pi \rightarrow \pi^*$  transition for the band located at 449 nm ( $\lambda_{\text{TD-DFT}}$   
11  
12 = 434 nm). Additionally, a small contribution of a MLCT can be observed. The NTOs for the  
13  
14 same absorption band calculated for the site ii Quercetin-Cu(II) complex ( $\lambda_{\text{TD-DFT}}$  = 419 nm)  
15  
16 also show that this transition is mainly  $\pi \rightarrow \pi^*$ . However, in this case a contribution of a ligand-  
17  
18 to-metal charge transfer (LMCT) is also observed. Since the NTO calculations are performed  
19  
20 under an unrestricted scheme, the  $\alpha$  and  $\beta$  spin orbitals are computed separately. However, both  
21  
22 spin orbitals are almost identical shape and energy for the transitions depicted in Figures 6 and 7,  
23  
24 except for the Quercetin-Cu(II) absorption band located at 381 nm. In this case, an ILCT/MLCT  
25  
26 mixed transition is observed for  $\alpha$ -spin orbitals (site i at  $\lambda_{\text{TD-DFT}}$  = 354 nm and site ii at  $\lambda_{\text{TD-DFT}}$  =  
27  
28 348 nm). The contribution of the  $\beta$ -spin orbitals is higher than the  $\alpha$ -spin and they show an  
29  
30 important LMCT in both complexation sites (Figure 8).  
31  
32  
33  
34  
35  
36  
37  
38  
39  
40  
41  
42  
43  
44  
45  
46  
47  
48  
49  
50  
51  
52  
53  
54  
55  
56  
57  
58  
59  
60

<i>i</i> -Quercetin-Cu(II)	Hole	Electron
T9( $\alpha$ ) $\lambda_{\text{TD-DFT}} = 434 \text{ nm}$ $f = 0.925$		
T27( $\alpha$ ) $\lambda_{\text{TD-DFT}} = 355 \text{ nm}$ $f = 0.168$		
<i>ii</i> -Quercetin-Cu(II)		
T12( $\alpha$ ) $\lambda_{\text{TD-DFT}} = 419 \text{ nm}$ $f = 1.182$		
T25( $\alpha$ ) $\lambda_{\text{TD-DFT}} = 348 \text{ nm}$ $f = 0.925$		

**Figure 7.** Contribution of the  $\alpha$ -spin orbitals for the *i*-Quercetin-Cu(II) and *ii*-Quercetin-Cu(II) complexes in the experimental absorption bands. For each state, the calculated wavelength ( $\lambda_{\text{TD-DFT}}$ ) and the oscillator strength  $f$  are listed.

<i>i</i> -Quercetin-Cu(II)	Hole	Electron
T27( $\beta$ ) $\lambda_{\text{TD-DFT}} = 355 \text{ nm}$ $f=0.168$		
<i>ii</i> -Quercetin-Cu(II)		
T25( $\beta$ ) $\lambda_{\text{TD-DFT}} = 348 \text{ nm}$ $f=0.925$		

**Figure 8.** Contribution of the  $\beta$ -spin orbitals for the *i*-Quercetin-Cu(II) and *ii*-Quercetin-Cu(II) complexes in the experimental absorption bands. For each state, the calculated wavelength ( $\lambda_{\text{TD-DFT}}$ ) and the oscillator strength  $f$  are listed.

#### 4. FT-IR RESULTS

The FT-IR spectra of the free ligands (Chrysin and Quercetin) and the metallic complexes were registered for determining some structural features of these compounds. The formation of the Chrysin-Cu(II) complex induces small changes in the spectrum of the flavonoid. The most important ones are the  $\nu(\text{C}=\text{O})$  vibration of Chrysin ( $1611 \text{ cm}^{-1}$ ) slightly shifted to a higher wavenumber in the complex ( $1616 \text{ cm}^{-1}$ ) and a band around  $619 \text{ cm}^{-1}$  in the Chrysin-Cu(II) spectrum disappears in the free ligand. This vibration can be attributed to the Cu-O stretching signal. Additionally, the relative intensity of the band at  $1275 \text{ cm}^{-1}$  associated with the coupled

1  
2  
3 vibrations  $\nu(\text{C-O})$  and  $\delta(\text{OH})$ <sup>48</sup> of free Chrysin is weakened in the complex spectrum. This may  
4  
5 be indicative that in the coordination site the deprotonated form of the flavonoid is involved.  
6  
7

8  
9 On the contrary, the complexation of Cu(II) ions by Quercetin induces important changes in the  
10  
11 vibrational spectrum. The most significant vibrational frequencies of Quercetin and its complex  
12  
13 are listed in Table 4 and the spectra are depicted in Figure 9. In the IR spectrum of the free  
14  
15 ligand the sharp bands located at 1667 and 1613  $\text{cm}^{-1}$  are assigned to the stretching modes of  
16  
17 C=O. In the metallic complex, a broad band appears around 1617  $\text{cm}^{-1}$ , indicating the  
18  
19 participation of this group in the coordination site. The strong band positioned at 1450  $\text{cm}^{-1}$  of  
20  
21 Quercetin, assigned to the  $\delta(\text{OH})$  vibrational mode<sup>49</sup>, notably reduces its intensity; also  
22  
23 suggesting the involvement of this group in the coordination site. The C–OH in plane  
24  
25 deformation band observed at 1265  $\text{cm}^{-1}$  in the free flavonoid shifts to 1296  $\text{cm}^{-1}$  in the complex,  
26  
27 which is usually observed when metal coordination involves the OH group<sup>31</sup>. The frequency  
28  
29 values for this band obtained from the vibrational analysis of DFT calculations are 1301  $\text{cm}^{-1}$   
30  
31 (site *i*) and 1319  $\text{cm}^{-1}$  (site *ii*). Finally, a new band (weak) can be found at 620  $\text{cm}^{-1}$  in the  
32  
33 complex spectrum, associated to the  $\nu(\text{Cu-O})$  vibrational mode<sup>50</sup>. The DFT vibrational  
34  
35 frequency for this vibration is located at 603  $\text{cm}^{-1}$  (site *i*) and 662  $\text{cm}^{-1}$  (site *ii*). These results also  
36  
37 supports site *i* as the preferential chelation site for the Quercetin-Cu(II) complex.  
38  
39  
40  
41  
42  
43  
44  
45  
46  
47  
48

49 **Table 4.** Selected experimental and theoretical (DFT) vibrational frequencies of Quercetin and  
50  
51 Quercetin-Cu(II) complex. The DFT frequencies were calculated at the UB3LYP/6-31+G(d,p)  
52  
53 and LANL2DZ level of theory and they are reported unscaled.  
54  
55  
56  
57  
58  
59  
60

Quercetin	Quercetin-Cu(II)	Quercetin-Cu(II) DFT		Assignments
		site <i>i</i>	site <i>ii</i>	
3616-2944	3665-3011	3444	3620	vO-H
1667				vC=O
1613	1617	1578	1578	vC=O, vC <sub>2</sub> =C <sub>3</sub>
1563	1558	1556	1519	v <sub>as</sub> (C <sub>2</sub> -C <sub>3</sub> -C <sub>4</sub> )
1265	1296	1301	1319	δ <sub>ip</sub> C-OH
1382	1363	1389	1400	δ <sub>ip</sub> C-OH, δ <sub>ip</sub> C-H, δO-H
1450, 1464	----	----	----	δOH, vC-O
867	879	853	857	α (ring)
----	620	603	662	vCu-O

α, planar ring deformation; δ, bending; v, stretching; as, asymmetric; ip, in-plane.

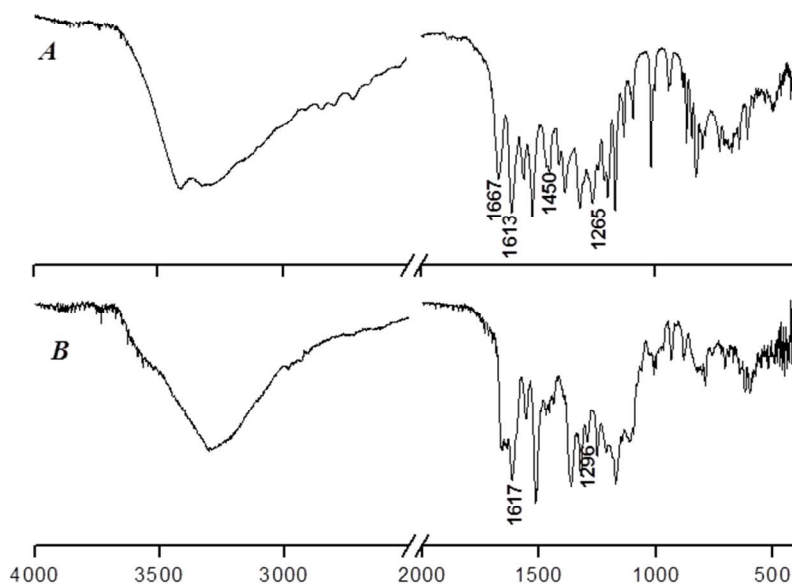


**Figure 9.** Infrared spectra of Quercetin (A) and its Cu(II) complex (B). The frequency axis is broken between 2500 and 2000  $\text{cm}^{-1}$ . No important bands have been observed in this region.

## CONCLUSIONS

In the present work, formation of two flavonoid-Cu(II) complexes in ethanolic solutions was studied. The studied systems were: Quercetin-Cu(II) and Chrysin-Cu(II). Both complexes presented 2:1 L:M stoichiometries, determined by Yoe-Jones method. The apparent stability constants were evaluated as Debattista *et al.* described. The standard enthalpy and entropy associated to the formation reaction were determined. These values show that the formation reactions are endothermic for both systems. The stability constants were also calculated from DFT analysis and they showed a good correlation with the experimental values. The TD-DFT calculations reproduces the main features of the analyzed complexes spectra and the results suggest that the 3-OH-4-oxo group is the preferred chelating site for Cu(II) ions in Quercetin under the adopted conditions. This observation is also supported with the analysis of the FTIR spectra. From a NTO analysis it is observed that Cu plays an important role in the UV-Vis absorption bands of the flavonoid complexes. The apparent formation constants for Quercetin-Cu(II) are higher than those of Chrysin-Cu(II) ones, suggesting that Quercetin may act as a better analytical reagent than Chrysin.

## AUTHOR INFORMATION

### Corresponding Author

\* Tel. +54 266 4520300 6617, e-mail address: mpaulina@unsl.edu.ar

## FUNDINGS

This work was developed thanks to contributions from Consejo Nacional de Investigaciones Científicas y Técnicas (CONICET) and Secretaría de Ciencia y Técnica of the Universidad Nacional de San Luis (SECyT UNSL), all in Argentine.

## REFERENCES

- (1) Casano, G.; Dumètre, A.; Pannecouque, C.; Hutter, S.; Azas, N.; Robin, M. Anti-HIV and Antiplasmodial Activity of Original Flavonoid Derivatives. *Bioorg Med Chem* **2010**, *18*, 6012–6023.
- (2) Sithisarn, P.; Michaelis, M.; Schubert-Zsilavec, M.; Cinatl, J. Differential Antiviral and Anti-Inflammatory Mechanisms of the Flavonoids Biochanin A and Baicalein in H5N1 Influenza A Virus-Infected Cells. *Antiviral Res* **2013**, *97*, 41–48.
- (3) Talia, J. M.; Tonn, C. E.; Debattista, N. B.; Pappano, N. B. Antibacterial Efficacy of Dihydroxylated Chalcones in Binary and Ternary Combinations with Nalidixic Acid and Nalidix Acid–Rutin Against *Escherichia Coli* ATCC 25 922. *Indian J Microbiol* **2012**, *52*, 638–641.
- (4) Navarro-Núñez, L.; Castillo, J.; Lozano, M. L.; Martínez, C.; Benavente-García, O.; Vicente, V.; Rivera, J. Thromboxane A2 Receptor Antagonism by Flavonoids: Structure-Activity Relationships. *J Agric Food Chem* **2009**, *57*, 1589–1594.
- (5) Khelifi, D.; Sghaier, R. M.; Amouri, S.; Laouini, D.; Hamdi, M.; Bouajila, J. Composition and Anti-Oxidant, Anti-Cancer and Anti-Inflammatory Activities of *Artemisia Herba-Alba*, *Ruta Chalpensis* L. and *Peganum Harmala* L. *Food Chem Toxicol* **2013**, *55*, 202–208.
- (6) Martin, M. A.; Goya, L.; Ramos, S. Potential for Preventive Effects of Cocoa and Cocoa Polyphenols in Cancer. *Food Chem Toxicol* **2013**, *56*, 336–351.
- (7) Xie, Y.-Y.; Qu, J.-L.; Wang, Q.-L.; Wang, Y.; Yoshikawa, M.; Yuan, D. Comparative Evaluation of Cultivars of *Chrysanthemum Morifolium* Flowers by HPLC-DAD-ESI/MS Analysis and Antiallergic Assay. *J Agric Food Chem* **2012**, *60*, 12574–12583.
- (8) Montaña, M. P.; Miskoski, S.; Criado, S.; Gianello, J. C.; Pappano, N.; Debattista, N.; García, N. A. Vitamin B2-Sensitized Photooxidation of Structurally Related Dihydroxyflavonoids. *Dye Pigment* **2003**, *58*, 113–120.

- 1  
2  
3 (9) Shiomi, K.; Kuriyama, I.; Yoshida, H.; Mizushina, Y. Inhibitory Effects of Myricetin on  
4 Mammalian DNA Polymerase, Topoisomerase and Human Cancer Cell Proliferation.  
5 *Food Chem* **2013**, *139*, 910–918.  
6  
7  
8 (10) Vitorino, J.; Sottomayor, M. J. DNA Interaction with Flavone and Hydroxyflavones. *J*  
9 *Mol Struct* **2010**, *975*, 292–297.  
10  
11 (11) Montaña, M. P.; Massad, W. A.; Criado, S.; Biasutti, A.; García, N. A. Stability of  
12 Flavonoids in the Presence of Riboflavin-Photogenerated Reactive Oxygen Species : A  
13 Kinetic and Mechanistic Study on Quercetin ,. *Photochem Photobiol* **2010**, *86*, 827–834.  
14  
15  
16 (12) Belobrajdic, D. P.; Bird, A. R. The Potential Role of Phytochemicals in Wholegrain  
17 Cereals for the Prevention of Type-2 Diabetes. *Nutr J* **2013**, *12*, 1–12.  
18  
19  
20 (13) Babich, H.; Schuck, A. G.; Weisburg, J. H.; Zuckerbraun, H. L. Research Strategies in the  
21 Study of the pro-Oxidant Nature of Polyphenol Nutraceuticals. *J Toxicol* **2011**, *2011*, 1–  
22 12.  
23  
24  
25 (14) Wang, S.-Q.; Han, X.-Z.; Li, X.; Ren, D.-M.; Wang, X.-N.; Lou, H.-X. Flavonoids from  
26 *Dracocephalum Tanguticum* and Their Cardioprotective Effects against Doxorubicin-  
27 Induced Toxicity in H9c2 Cells. *Bioorg Med Chem Lett* **2010**, *20*, 6411–6415.  
28  
29  
30 (15) Xiao, Z.-P.; Peng, Z.-Y.; Dong, J.-J.; He, J.; Ouyang, H.; Feng, Y.-T.; Lu, C.-L.; Lin, W.-  
31 Q.; Wang, J.-X.; Xiang, Y.-P.; Zhu, H.-L. Synthesis, Structure-Activity Relationship  
32 Analysis and Kinetics Study of Reductive Derivatives of Flavonoids as *Helicobacter*  
33 *Pylori* Urease Inhibitors. *Eur J Med Chem* **2013**, *63*, 685–695.  
34  
35  
36 (16) Barbarić, M.; Mišković, K.; Bojić, M.; Lončar, M. B.; Smolčić-Bubalo, A.; Debeljak, Z.;  
37 Medić-Šarić, M. Chemical Composition of the Ethanolic Propolis Extracts and Its Effect  
38 on HeLa Cells. *J Ethnopharmacol* **2011**, *135*, 772–778.  
39  
40  
41 (17) Kim, D.-C.; Rho, S.-H.; Shin, J.-C.; Park, H. H.; Kim, D. Inhibition of Melanogenesis by  
42 5,7-Dihydroxyflavone (chrysin) via Blocking Adenylyl Cyclase Activity. *Biochem*  
43 *Biophys Res Commun* **2011**, *411*, 121–125.  
44  
45  
46 (18) Ferrari, G. V; Pappano, N. B.; Debattista, N. B.; Montan, M. P. Potentiometric and  
47 Spectrophotometric Study of 3-Hydroxyflavone-La ( III ) Complexes. *J Chem Eng Data*  
48 **2008**, *53*, 1241–1245.  
49  
50  
51 (19) Ferrari, G. V; Pappano, N. B.; Montaña, M. P.; García, N. A.; Debattista, N. B. Novel  
52 Synthesis of 3,3 ' -Dihydroxyflavone and Apparent Formation Constants of Flavonoid-Ga  
53 ( III ) Complexes. *J Chem Eng Data* **2010**, *55*, 3080–3083.  
54  
55  
56 (20) De Souza, R. F. V; De Giovani, W. F. Synthesis, Spectral and Electrochemical Properties  
57 of Al(III) and Zn(II) Complexes with Flavonoids. *Spectrochim Acta A Mol Biomol*  
58 *Spectrosc* **2005**, *61*, 1985–1990.  
59  
60



- 1  
2  
3  
4  
5  
6  
7  
8  
9  
10  
11  
12  
13  
14  
15  
16  
17  
18  
19  
20  
21  
22  
23  
24  
25  
26  
27  
28  
29  
30  
31  
32  
33  
34  
35  
36  
37  
38  
39  
40  
41  
42  
43  
44  
45  
46  
47  
48  
49  
50  
51  
52  
53  
54  
55  
56  
57  
58  
59  
60
- (21) Bukhari, S. B.; Memon, S.; Tahir, M. M.; Bhangar, M. I. Synthesis , Characterization and Investigation of Antioxidant Activity of Cobalt – Quercetin Complex. *J Mol Struct* **2008**, *892*, 39–46.
- (22) AL-Kindy, S. M. Z.; Al-Hinai, K. H.; Suliman, F. E. O.; Al-Lawati, H. J.; Pillay, A. Development of a Selective Fluorimetric Technique for Rapid Trace Determination of Zinc Using 3-Hydroxyflavone. *Arab J Chem* **2011**, *4*, 147–152.
- (23) Ravichandran, R.; Rajendran, M.; Devapiriam, D. Antioxidant Study of Quercetin and Their Metal Complex and Determination of Stability Constant by Spectrophotometry Method. *Food Chem* **2014**, *146*, 472–478.
- (24) Chen, W.; Sun, S.; Cao, W.; Liang, Y.; Song, J. Antioxidant Property of quercetin–Cr(III) Complex: The Role of Cr(III) Ion. *J Mol Struct* **2009**, *918*, 194–197.
- (25) Baccan, M. M.; Chiarelli-Neto, O.; Pereira, R. M. S.; Espósito, B. P. Quercetin as a Shuttle for Labile Iron. *J Inorg Biochem* **2012**, *107*, 34–39.
- (26) Paradelo, M.; Letzner, A.; Arias-Estévez, M.; Garrido-Rodríguez, B.; López-Periago, J. E. Influence of Soluble Copper on the Electrokinetic Properties and Transport of Copper Oxochloride-Based Fungicide Particles. *J Contam Hydrol* **2011**, *126*, 37–44.
- (27) Dong, J.; Chen, S.; Corti, D. S.; Franses, E. I.; Zhao, Y.; Ng, H. T.; Hanson, E. Effect of Triton X-100 on the Stability of Aqueous Dispersions of Copper Phthalocyanine Pigment Nanoparticles. *J Colloid Interface Sci* **2011**, *362*, 33–41.
- (28) Emekli, U.; West, A. C. Simulation of Electrochemical Nucleation in the Presence of Additives under Galvanostatic and Pulsed Plating Conditions. *Electrochim Acta* **2010**, *56*, 977–984.
- (29) Fixman, E. M.; Abello, M. C.; Gorriz, O. F.; Arru, L. A. Preparation of Cu / SiO<sub>2</sub> Catalysts with and without Tartaric Acid as Template via a Sol – Gel Process Characterization and Evaluation in the Methanol Partial Oxidation. *Appl Catal A Gen* **2007**, *319*, 111–118.
- (30) Peñarrubia, L.; Romero, P.; Carrió-Seguí, A.; Andrés-Bordería, A.; Moreno, J.; Sanz, A. Temporal Aspects of Copper Homeostasis and Its Crosstalk with Hormones. *Front Plant Sci* **2015**, *6*, 1–18.
- (31) Pękal, A.; Biesaga, M.; Pyrzynska, K. Interaction of Quercetin with Copper Ions: Complexation, Oxidation and Reactivity towards Radicals. *Biometals* **2011**, *24*, 41–49.
- (32) Sawyer, D. T.; Heinman, W. R.; Beebe, J. M. *Chemistry Experiments for Instrumental Methods*; John Wiley & Sons: New York, 1984.

- 1  
2  
3 (33) Debattista, N. B.; Pappano, N. B. Aluminium ( III ) and Substituent ' S Effect. *Talanta*  
4 **1997**, *44*, 1967–1971.  
5  
6  
7 (34) Becke, a. D. Density-Functional Exchang-Energy Approximation with Correct  
8 Asymptotic Behavior. **1988**, *38*, 3098–3100.  
9  
10 (35) Lee, C.; Yang, W.; Parr, R. G. Into a Functional of the Electron Density F F. *Phys Rev B*  
11 **1988**, *37*, 785–789.  
12  
13 (36) Cancès, E.; Mennucci, B.; Tomasi, J. A New Integral Equation Formalism for the  
14 Polarizable Continuum Model: Theoretical Background and Applications to Isotropic and  
15 Anisotropic Dielectrics. *J Chem Phys* **1997**, *107*, 3032.  
16  
17 (37) Stratmann, R. E.; Scuseria, G. E.; Frisch, M. J. An Efficient Implementation of Time-  
18 Dependent Density-Functional Theory for the Calculation of Excitation Energies of Large  
19 Molecules. *J Chem Phys* **1998**, *109*, 8218–8224.  
20  
21 (38) Ernzerhof, M.; Scuseria, G. E. Assessment of the Perdew-Burke-Ernzerhof Exchange-  
22 Correlation Functional. *J Chem Phys* **1999**, *110*, 5029–5036.  
23  
24 (39) Adamo, C.; Barone, V. Toward Reliable Density Functional Methods without Adjustable  
25 Parameters: The PBE0 Model. *J Chem Phys* **1999**, *110*, 6158.  
26  
27 (40) Zhao, Y.; Truhlar, D. G. The M06 Suite of Density Functionals for Main Group  
28 Thermochemistry, Thermochemical Kinetics, Noncovalent Interactions, Excited States,  
29 and Transition Elements: Two New Functionals and Systematic Testing of Four M06-  
30 Class Functionals and 12 Other Function. *Theor Chem Acc* **2008**, *120*, 215–241.  
31  
32 (41) Yanai, T.; Tew, D. P.; Handy, N. C. A New Hybrid Exchange-Correlation Functional  
33 Using the Coulomb-Attenuating Method (CAM-B3LYP). *Chem Phys Lett* **2004**, *393*, 51–  
34 57.  
35  
36 (42) Martin, R. L. Natural Transition Orbitals. *J Chem Phys* **2003**, *118*, 4775–4777.  
37  
38 (43) Frisch, M. J., Trucks, G. W., Schlegel, H. B., Scuseria, G. E., Robb, M. A., Cheeseman, J.  
39 R., Scalmani, G., Barone, V., Mennucci, B., Petersson, G. A., Nakatsuji, H., Caricato, M.,  
40 Li, X., Hratchian, H. P., Izmaylov, A. F., Bloino, J., Zheng, G., Sonnenb, D. J. Gaussian  
41 09, 2013.  
42  
43 (44) Ferrari, G. V; Paulina Montaña, M.; Dimarco, F. C. D.; Debattista, N. B.; Pappano, N. B.;  
44 Massad, W. A.; García, N. A. A Comparative Photochemical Study on the Behavior of  
45 3,3'-Dihydroxyflavone and Its Complex with La(III) as Generators and Quenchers of  
46 Reactive Oxygen Species. *J Photochem Photobiol B* **2013**, *124*, 42–49.  
47  
48  
49  
50  
51  
52  
53  
54  
55  
56  
57  
58  
59  
60

- 1  
2  
3  
4  
5  
6  
7  
8  
9  
10  
11  
12  
13  
14  
15  
16  
17  
18  
19  
20  
21  
22  
23  
24  
25  
26  
27  
28  
29  
30  
31  
32  
33  
34  
35  
36  
37  
38  
39  
40  
41  
42  
43  
44  
45  
46  
47  
48  
49  
50  
51  
52  
53  
54  
55  
56  
57  
58  
59  
60
- (45) Matulis, V. E.; Halauko, Y. S.; Ivashkevich, O. a.; Gaponik, P. N. CH Acidity of Five-Membered Nitrogen-Containing Heterocycles: DFT Investigation. *J Mol Struct THEOCHEM* **2009**, *909*, 19–24.
- (46) Moncomble, A.; Cornard, J.-P. Elucidation of Complexation Multi-Equilibrium with Mg<sup>II</sup> and a Multisite Ligand. A Combined Electronic Spectroscopies and DFT Investigation. *RSC Adv* **2014**, *4*, 29050.
- (47) Furia, E.; Marino, T.; Russo, N. Insights into the Coordination Mode of Quercetin with the Al(III) Ion from a Combined Experimental and Theoretical Study. *Dalt Trans* **2014**, *43*, 7269.
- (48) Uivarosi V., Badea M., Olar R., Drăghici C., Bărbuceanu Ș. F. Synthesis and Characterization of Some New Complexes of Magnesium (II) and Zinc (II) with the Natural Flavonoid Primuletin. *Molecules* **2013**, *18*, 7631.
- (49) Ansari A. <sup>1</sup>H NMR and spectroscopic studies of biologically active yttrium (III)-flavonoid complexes. *Main Group Chem.* **2008**, *7*, 133.
- (50) Nakamoto K. *Infrared and Raman Spectra of Inorganic and Coordination Compounds. Part B*, fifth ed.; Wiley-Interscience: New York, 1997.

## TABLE OF CONTENTS GRAPHIC

